



Performance Evaluation of Regular Hexagonal Pyramid Three-Dimensional Solar Desalination System: An Experimental Investigation

Seyed Alireza Alamshah^a, Mohsen Talebzadegan^{a*}, Mojtaba Moravej^b

^aDepartment of Mechanical Engineering, Ahvaz Branch, Islamic Azad University, Ahvaz, Iran.

^bDepartment of Mechanical Engineering, Payame Noor University, Tehran, Iran.

ARTICLE INFO

Article Type:

Research Article

Received:03.01.2024

Accepted:13.09.2024

Keywords:

Solar desalination,
Hexagonal pyramid,
Experimental,
Performance,
Three-Dimensional

ABSTRACT

In this study, a solar desalination unit with a regular hexagonal pyramid geometry was designed, constructed, and investigated. The unit was built as a hexagonal pool made of 2 mm thick iron, with an absorption surface of 1 square meter, and covered with 4 mm thick glass. It was tested under the weather conditions in Ahvaz City, southwest Iran. In its baseline and inactive state, without any performance-enhancing measures, the solar desalination unit could produce more than 3 liters of freshwater per square meter of the absorption surface daily under summer weather conditions. The changes in the production rate relative to the intensity of solar radiation and the temperature of the saltwater pool were examined. The solar desalination unit produced more freshwater during midday and afternoon hours, when the air temperature was higher. The thermal efficiency of the device was 27.1%, comparable to similar studies. Also, the effect of wind speed and relative humidity of the ambient air on fresh water production was investigated.

1. Introduction

Solar energy is one of the most well-known and practical forms of renewable energy, with applications in both solar heat and solar electricity. Solar radiation is converted into energy in solar heating systems and transferred to power plants, water heaters, and desalination units [1-5].

Researchers worldwide have been studying solar-powered desalination systems that use only solar radiation to evaporate saltwater and other non-potable water sources, and then condense the steam to produce distilled, drinkable water. However, many factors can influence the efficiency of these systems and the amount of potable water they produce. To increase freshwater production,

*Corresponding Author Email: talebzadegan.m@gmail.com

Cite this article: Alamshah, S. A., Talebzadegan, M., & Moravej, M. (2024). Performance Evaluation of Regular Hexagonal Pyramid Three-Dimensional Solar Desalination System: An Experimental Investigation. *Journal of Solar Energy Research*, 9(2), 1914-1925. doi: 10.22059/jsr.2024.370071.1371

DOI: 10.22059/jsr.2024.370071.1371



scientists and researchers worldwide are attempting to enhance the efficiency of solar desalination systems by changing their geometry, using new and more efficient materials, combining solar energy with other energy sources, or employing more complex equipment. Identifying factors that can increase the efficiency and productivity of these desalination systems requires further research. In traditional solar desalination devices, a water tank absorbs solar radiation within a completely closed volume, producing water vapor that condenses on a sloping, transparent surface and is eventually collected as potable freshwater. Humans have employed this straightforward method since ancient times to produce drinking water from seawater or brackish water. The rate of freshwater production varies significantly across different designs and regions. In their study [6], Abd Elbar and Hassan combined single-sided solar desalination with a solar energy absorber panel. They aimed to enhance the desalination process efficiency by preheating saltwater before it entered the desalination chamber. They used black steel fibers as a porous material to increase the system efficiency. The solar desalination reservoir measured 100×100 cm, with sloping glass walls of 100×120 cm at a 31° angle. They found that preheating saltwater by 40%, 50%, and 60% increased freshwater production by 10.4%, 15.5%, and 20.9% and improved the system efficiency by 8.2%, 13%, and 20%, respectively.

Zanganeh et al. [7] evaluated the impact of changing the transparent tilted surface cover on the production rate of a single-sided solar desalination system. The system had a reservoir size of 50×50 cm² and was tested at three different tilt angles of 25° , 35° , and 45° . The tilted cover inner surface was coated with silicon and titanium dioxide nanoparticles. They found that using titanium dioxide at a 25° angle increased the desalination process efficiency. They also realized that increasing the tilt angle to 35° and 45° for the surface covered with silicon nanoparticles resulted in higher condensed water production compared to the uncovered surface and the surface covered with titanium dioxide. In another study, Modi and Nayi [8] investigated the effects of forced evaporation and condensation on a four-sided pyramid-shaped solar desalination system with heat storage materials. The system measured 50×50 cm² had a glass installation angle of 20° . They conducted the study in three stages. In the first stage, they used black graphite as a thermal energy storage material at depths of 20 mm and 30 mm in saltwater, producing 1.430 liters of freshwater per square meter. Using

thermal energy storage materials at a depth of 30 mm increased the production rate by 13.96%. In the second stage, they compared forced distillation with forced evaporation, resulting in a 33.24% increase in freshwater production rate. In the third stage, they combined forced evaporation with thermal energy storage materials at a depth of 30 mm in saltwater, obtaining a production rate of 2.253 liters of freshwater per square meter. This combination led to a 61.48% increase in production compared to the mechanism without thermal energy storage materials and forced evaporation. Additionally, they observed that the rate of freshwater production, device efficiency, and economic savings of the project were higher in the third stage compared to the other stages. Saravanan and Murugan [9] investigated the effects of using woolen, knitted hemp, cotton, and polyester fabrics to enhance the evaporation surface in a solar desalination system. The system had a pyramid shape, measuring 50×50 cm², with four triangular glass covers placed at a 45° angle relative to the saltwater tank surface. They found that using these fabrics in the saltwater pool at a depth of 2 cm increased the rate of freshwater production by 14.4%, 23.1%, 21.2%, and 29.6%, respectively, compared to using the fabrics at depths of 3, 4, 5, and 6 cm. Radomska et al. [10] modeled and investigated the thermal processes of a solar desalination system. To this end, a pool was built with a 0.8 mm thick stainless-steel sheet, covered with a 4 mm glass at a 30° angle to the horizon. The experiment was conducted at saltwater depths of 2, 3, and 4 cm with three different solar radiation power levels, modeled using electric heaters. The results showed that saltwater depth significantly affected the device efficiency, and this effect increased by decreasing solar radiation power. Furthermore, the maximum freshwater volume produced at a saltwater depth of 2 cm was 800, 3722, and 9292 milliliters per square meter per day for low, medium, and high solar radiation power levels, respectively. Additionally, reducing the depth of saltwater from 4 to 3 cm resulted in 7.3%, 8.7%, and 7.5% increases in freshwater production for low, medium, and high solar radiation power levels, respectively. Poonia et al. [11] investigated the design and performance of solar desalination equipment with solar concentrators in the hot country of India. They designed and assembled a solar desalination device with a hemispherical concentrator and an evaporation chamber at the center. The hemispherical concentrator with a diameter of 2.6 meters and an efficiency of over 700 watts increased the temperature at the focal point

and the production temperature center to about 350° C. The average daily efficiency was 24.2% in May and 32.3% in December, with a maximum hourly output of 0.85 liters.

In a practical experiment, Abed et al. [12] investigated the effects of operating conditions and design on a solar desalination unit equipped with a concentrator and heater in the climate of Iraq. They used oil as a secondary fluid in a closed circuit to heat the water in the solar desalination chamber. The design included two hemispherical concentrators, each with a diameter of 143 cm and covered with aluminum sheets, and a cylindrical stainless-steel tank with a diameter of 20 cm, installed at the center of the concentrators in Tikrit, Iraq. The results showed that the simultaneous use of two concentrators almost doubled freshwater production. With the use of one concentrator, the daily output was 18.4 liters of freshwater, while using two concentrators increased this amount to 30.97 liters per day. Muthu Manokar et al. [13] studied the design and construction of a hemispherical solar desalination device in both active and passive modes. For the passive sample, a triangular metal tank with an area of 0.25 m² was designed and covered with tilted transparent acrylic sheets for water vapor condensation. The active sample was designed similarly but included a solar heater with either a straight or spiral tube. Comparative analysis of the active and passive modes confirmed that using a solar heater with straight and spiral tubes at the lowest water flow rate of 0.00039 kg/s led to an increase in the daily average temperature of the desalinated water by 14.15% and 11.36%, respectively. The results also showed that the active water desalination system equipped with a spiral tube heater obtained the maximum daily production rate, thermal efficiency, and exergy efficiency, with values of 6.35 kg/m², 13.03%, and 2.61%, respectively, at the minimum water rotational flow rate. Kabeel et al. [14] conducted a study to determine the effect of the placement angle of the glass cover on the performance of a four-sided pyramid-shaped solar water desalination device. They designed and constructed three prototypes with the glass roof installed at angles of 30.47°, 40°, and 50°. The productivity of the device was examined under different conditions. The desalination device achieved the highest thermal efficiency and water production rate when the glass angle matched the geographical latitude of the test site. Solar energy absorption was highest at a 30.47° angle for the glass roof. The water production rate was measured at 4.13 liters per day per square meter for the 30.47°

angle of the glass, 3.5 liters per day per square meter for the 40° angle, and 2.93 liters per day per square meter for the 50° angle. In their experimental study, Chaichan et al. [15] designed an inexpensive solar desalination device that could meet the drinking water requirements of a household in Oman using a simple and cost-effective method. The designed system comprised a glass box, a metal pot, a glass container, mirror components, and a large stainless steel pot for collecting the produced freshwater. The device was tested with seawater, pipeline water, and wastewater as water samples. Notably, the chemical and health characteristics of the freshwater produced from all three water samples met human drinking water standards. The system, measuring 66 × 28 cm, had a freshwater production capacity of 1 to 4 liters per day. Sankaran and Sirdinharan [16] investigated the simulation of evaporation and condensation processes in desalination units by examining a three-dimensional model. In this study, they simulated a conventional passive solar distillation system with two slopes using ANSYS Fluent software and compared the results with experimental data. The final results demonstrated a good match between the theoretical and experimental findings. In another study, Shakerian et al. [17] developed a solar desalination unit for groundwater sources. To this end, they constructed an experimental solar distillation unit to analyze the effects of orientation, water pool depth, weather conditions, input salinity, and flow rate on the unit's performance. The results showed that the unit had the highest efficiency when the water pool had a depth of 3 cm. Kumar et al. [18] investigated a solar desalination system enhanced by ceramic nanoparticles. They reported an efficiency of about 34% for the device and 22% for a conventional desalination system. Naghdi et al. [19] designed, built and tested a salt-resistant solar water desalination system. In the above system, they used a surface hydration layer to remove salt and then evaluated it experimentally. The results of the study showed that this system has a better performance compared to the previous systems and the performance rate is about 86%. Senthilkumar et al. [20] conducted an interesting research on a solar water desalination plant that was filled by gravel and granite in terms of volume. The results of the research showed an increase in the amount of water evaporation even in cases where there was little sunlight. Also, a deviation of 6.58% was reported in the difference between the use of gravel and granite. Ramy et al. [21] used a new hybridization method to increase desalination and desalination in the production of desalinated water. The models used in

combination were also examined from an economic point of view. The results of the research showed that both the amount of desalination has improved by about 30% and the costs have decreased between 23 and 27%. Zhang et al. [22] used a two-layer hydrogen solar evaporation system for desalination. In their investigations, it was found that the evaporation rate of water reaches 2.77 kg/m², which is suitable and practical for water purification, especially on a large scale.

In the present study, in order to increase the receiving of solar radiation in a three-dimensional form and to provide a solar water desalination with an independent and stable geometry, as well as to improve performance, a pyramid solar water desalination was designed and built by authors and tested experimentally.

2. Materials and Methods

The current experiment aims to produce fresh water from salt water using only solar energy, without advanced or expensive equipment. This is solely based on the traditional method of saltwater evaporation and steam condensation in the Ahvaz region's climate. The experiment examines the effect of receiving solar radiation from various directions on the device's production rate. To achieve this, the device is designed to allow sunlight radiation to shine on the energy-absorbing basin from all directions without any obstruction. Instead of being followed by the device's solar tracking devices, the possibility of absorbing and receiving radiation from any direction by the device in a fixed position is provided. To achieve this, the device is designed and constructed as a hexagonal pyramid. The device's chamber, the solar thermal energy absorber, is a hexagonal reservoir filled with salt water and exposed to radiation. A sloping condensing surface is formed on the chamber by placing a sloping glass roof and sealing the space inside the control volume.

The condensed water flows down the glass and is collected in a channel encircling the upper edge of the basin that collects fresh water and directs it towards the outlet. The chamber has three openings for the inflow of saltwater and outflow of fresh water, as well as a pathway for discharging and washing saltwater built into the walls of the chamber. The source of saltwater, situated at a higher elevation than the chamber outside the desalination device, is responsible for supplying saltwater and compensating for the water level shortfall in the chamber. Saltwater flows into the chamber from the source through the force of

gravity. A floating valve is installed inside the chamber and maintains the depth of the saltwater at a constant level. The outlet for fresh water from the device is poured into a plastic graduated container to measure continuously according to the experimental procedure. Table 1 displays the device's technical specifications, while Figure 1 depicts the layout of the various parts of the experiment. In Table 2, the physical specifications required for effective parameters are presented. The device produces fresh water into the plastic reservoir. The desalination device's chamber is insulated to eliminate heat losses on the bottom and walls and is placed on a stand 50 centimeters away from the ground surface. The water flows between the saltwater reservoir, the solar desalination device basin, and the freshwater collection reservoir through short plastic hoses too small to have significant heat exchange effects, as illustrated in Figure 2. Environmental and solar parameters were separately measured using the devices listed in Table 3 to accurately measure the device's performance.

Table 1. Technical Specifications, Dimensions, Sizes of Parts, and Consumables.

Specification	Description
2mm black iron sheet	The body of the device's chamber
4mm plain glass	The transparent and sloping ceiling of the chamber
12-density Styrofoam with 30mm thickness	Insulation of the body of the chamber
1/2 inches transparent plastic hose	Connecting pipes
3/8 inches copper pipe	freshwater output pipe from the device
Aquarium silicone adhesive and transparent tape	Waterproof adhesive
1 square meter	The total area of the absorbent
1.2 square meters	The total surface area of the condenser
Aluminum profiled flange	Drain channel for potable water discharge
5-liter plastic tank	saltwater supply tank

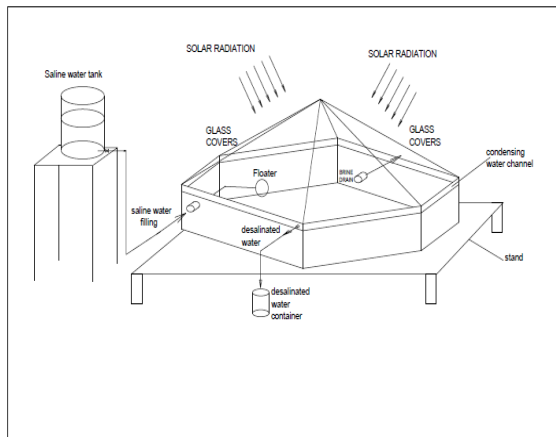


Figure 1. Experimental Setup Schematic

Table 2. Coefficient Values Used in Calculations[14]

Parameter	Value
Pool dimensions	1 square meter
Glass transmission coefficient	$\tau_g = 0.9$
Water transmission coefficient	$\tau_w = 0.8$
Internal surface absorption coefficient	$p = 0.9 \alpha$
Water evaporation latent heat	$h_{fg} = 2256 \text{ kJ/kg}$



Figure 2. Desalination pyramid device under testing

Table 3. Measurement instruments specifications

Instrument Name	Model	Unit	Measurement Accuracy
Thermometer	DL7105	°C	±0.1

Solar radiation meter	TES1333	W/m ²	±1
freshwater volume meter	Graduated cylinder 500	mL	±0.5
Hygrometer	DC103	%	±1
Anemometer	LUTRON	m/s	±0.1

2.1. Governing Equation:

A solar desalinator with a pyramid shape and a glass cover on the saltwater pool is explained in terms of thermal conditions. The pool has a dark surface, and its purpose is to absorb solar energy, increasing water temperature inside the pool. The black and matte color inside the pool helps achieve this goal. In the figure below, we can observe the hypothetical control volume surrounding the solar desalinator and the effective energy components on this control volume.

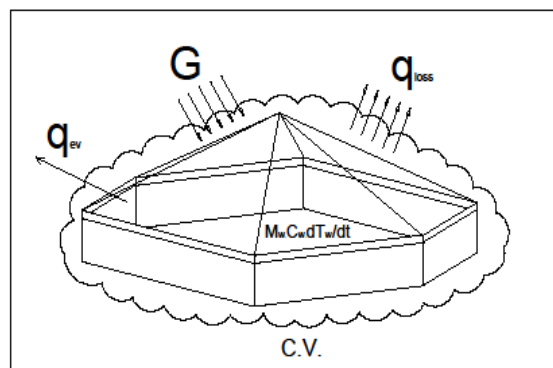


Figure 3. Control volume of the device

The energy balance equation for the control volume shown in the above figure is as follows [14]:

$$\sum \dot{E}_{in} - \sum \dot{E}_{out} = \dot{E}_{st} \tag{1}$$

The equation above includes $\sum \dot{E}_{in}$, which represents the input energy rates to the control volume, $\sum \dot{E}_{out}$, which represents the output energy rates from the control volume, and $\sum \dot{E}_{st}$, which represents the energy change rate within the control volume. By replacing various energy components with equation (2), we can obtain [14].

$$\tau_w \alpha_p GA - q_{ev} = M_w C_w \frac{\Delta T_w}{\Delta t} \quad (2)$$

In Equation (2), G represents the solar radiation intensity measured in (W/m²). The rate of evaporative heat transfer is denoted as q_{ev}, the rate of heat loss from the control volume as q_{loss}, the mass of saltwater as M_w, the specific heat capacity of saltwater as C_w, the temperature change of the pool as ΔT_w, the time interval as Δt, the absorber plate area as A, the absorber plate absorptivity coefficient as α_p, the transmissivity coefficient of salt water inside the pool as τ_w, and the transmissivity coefficient of the glass cover as τ_g. The rate of heat loss from the control volume includes convective and radiative losses from the freshwater within the desalination device. The rate of evaporative heat transfer from the control volume can be obtained from the following Equation [14]:

$$q_{ev} = \frac{m_w \cdot L_f}{\Delta t} \quad (3)$$

In Equation (3), m_w refers to the quantity of produced freshwater, and L_f represents the latent heat of water evaporation. Moreover, understanding the system's efficiency aids in its better operation and implementing effective changes for improved performance. A system's efficiency is typically expressed as the ratio of output work or energy to input work or energy, as shown in equation (4).

$$\eta = \frac{Q_u}{E_{in}} \quad (4)$$

The six-sided solar still device is no exception to this rule. The ratio of the desired energy output rate, q_{ev}, to the net energy input rate, which is the amount of solar energy reaching the device, can be determined by using Equation (6) to calculate the thermal efficiency of the solar desalination device, as presented in Equation (7) [14].

$$Q_u = q_{ev} \quad (5)$$

$$E_{in} = GA \quad (6)$$

In this equation, G represents the solar radiation intensity in (W/m²), while A is the area that receives the radiation. Since the absorber area is one square meter, we can use the above equation to obtain the following [14]:

$$\eta = \frac{q_{ev}}{G} \quad (7)$$

Equation (7) demonstrates the efficiency at the exact moment when measurements are taken. Meanwhile, Equation (8) computes the device's overall efficiency from the start of the experiment up

to time t. It's evident that when t equals the end time of the experiment, the device's daily efficiency is obtained [14].

$$\eta_{total} = \frac{\sum_0^t m \cdot L_f}{\sum_0^t G \cdot t} \quad (8)$$

2.2. Uncertainty Analysis

In general, many experimental tests and research studies are not immune to errors and can have multiple uncertainties. The critical point is that the researcher must strive to minimize the level of uncertainty and provide a better understanding of the results of their research by measuring the level of uncertainty. In this study, the measurement of uncertainty in the efficiency of this desalination unit is required using Equation (7). The RMSS method is used to evaluate the analysis, and Equation (9) is employed to calculate the uncertainty in measuring the efficiency of the desalination unit for several measured parameters [14].

$$s_u = \left(\sum_{i=1}^n \left[a_i \frac{\partial u_i}{\partial x_i} \right] \right)^{1/2} \quad (9)$$

Where u is a function of multiple parameters, namely x, and a is its coefficient. If the function being evaluated has a multiplier of 1, i.e., a_i = 1, from independent data, then the uncertainty of this function will be calculated as Equation (10)[14].

$$S_u = \sqrt{\left(\frac{\Delta u_1}{u_1}\right)^2 + \left(\frac{\Delta u_2}{u_2}\right)^2 + \left(\frac{\Delta u_3}{u_3}\right)^2 + \dots} \quad (10)$$

Considering the significance of the key quantities in this study, which include the efficiency of the solar desalination unit and its performance, equation (8) can be expressed as Equation (10) based on Equation (7) for the desalination unit's efficiency [14].

$$S_\eta = \sqrt{\left(\frac{\Delta m}{m}\right)^2 + \left(\frac{\Delta DT}{T}\right)^2 + \left(\frac{\Delta G_T}{G_T}\right)^2} \quad (11)$$

The level of uncertainty measured for this study is approximately 5.5%, based on the data obtained from Table 4.

Table 4. Uncertainty of experimental data

Parameter Name	Uncertainty Level (%)
Temperature	1.3%
Solar radiation	4.7%
Water mass	1%

3. Results and discussion

The experiment was carried out in Ahvaz city in August 2022 after the device was completely prepared and drained one hour prior to the start of the test. The test was conducted from 8:30 AM to 6:30 PM and then repeated under new weather and temperature conditions. During the test period, which was recorded in 15-minute intervals, temperatures, solar radiation intensity, environmental parameters, and the amount of freshwater production were all monitored and recorded. Figure 4 displays the variations in radiation intensity throughout the experiment. The parameter values, expressed in watts per square meter, began at 455 W/m² at the start of the test when the solar radiation angle was inclined and early in the day. It peaked at 1129 W/m² at 2 PM and gradually decreased for the remainder of the experiment, consistently declining in the final hours. Since the power obtained from solar radiation is the most influential factor in the amount of freshwater produced by the solar desalination system, the device's freshwater production is expected to increase during periods with higher levels of solar radiation energy. Figure 5 shows the wind speed, while Figure 6 displays the relative humidity of the surrounding ambient air, measured and presented during the experiment.

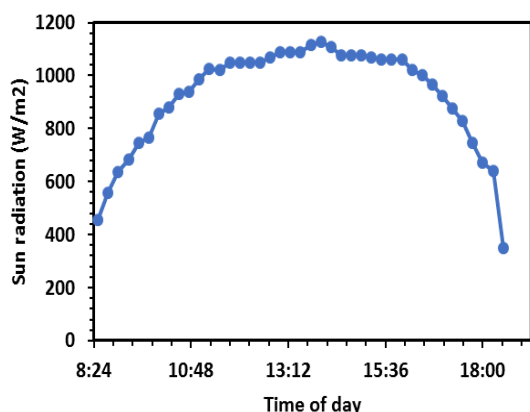


Figure 4. The solar radiation received by the solar desalination system during the experiment

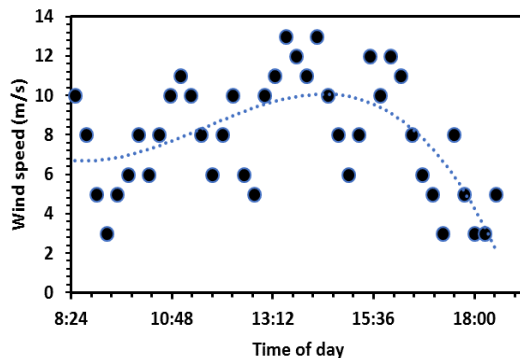


Figure 5. The wind speed in the environment surrounding the device during the experiment

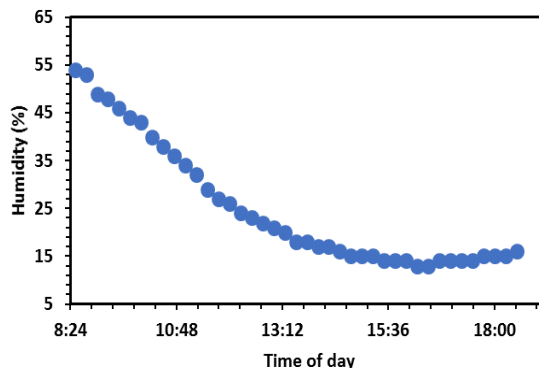


Figure 6. The level of relative humidity of the ambient air during the test

The wind speed during the experiment was relative and repeatedly fluctuated, reaching a minimum of 2 m/s and sometimes exceeding 12 m/s in specific directions, as demonstrated in Figure 4. In Figure 5, the ambient air humidity followed a particular pattern and decreased throughout the experiment. Figure 7 displays the changes in ambient air temperature, which consistently increased from morning until the afternoon before starting to decline. The temperature of the saline water inside the device and the glass wall of the desalination unit were also presented. Although they were initially at the same temperature, due to increased radiation and greenhouse effects, the glass wall and water temperature gradually exceeded the ambient temperature, which is inherent to the device's nature. In Figure 8, the graph illustrates the quantity of water produced at the outlet of the desalination unit throughout the experiment. The graph shows the amount of water produced in 15-minute intervals and the total amount made from the start until that specific moment. As depicted in the graph, the quantity of produced water varies at different moments due to changes in environmental conditions, and it has fluctuated in some minutes.

Nonetheless, the significant point is that both cumulative and momentary water production has increased with time.

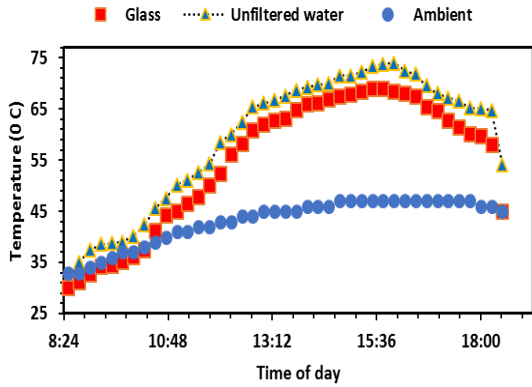


Figure 7. The ambient air temperature, the temperature of the glass wall, and the saline water inside the device during the experiment

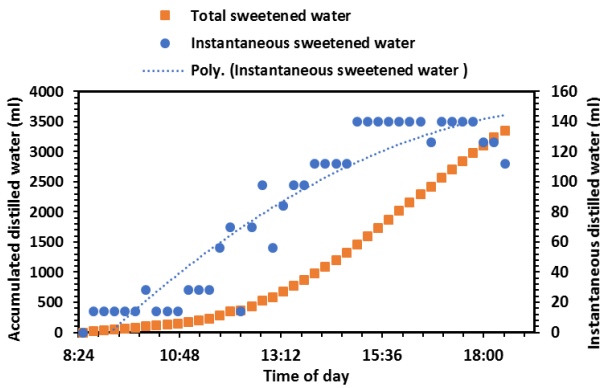


Figure 8. The amount of water produced in both momentary and cumulative forms during the experiment

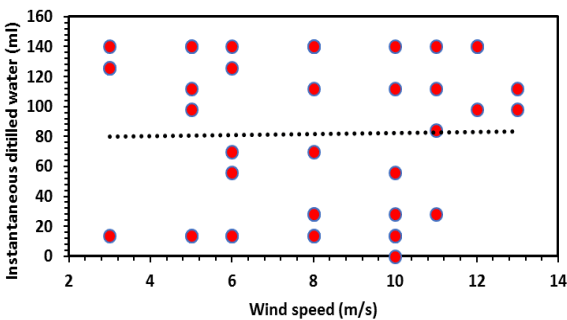


Figure 9. The effect of wind speed on the amount of desalinated water

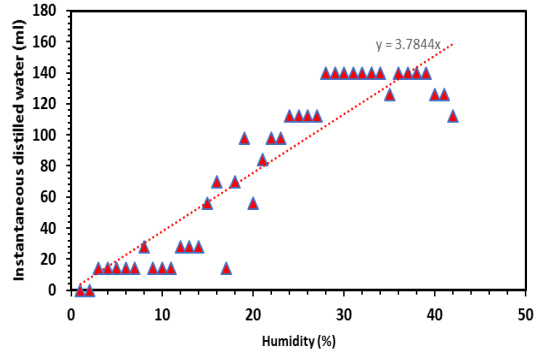


Figure 10. The effect of air humidity on the amount of desalinated water

Figures 9 and 10 display the momentary production of freshwater based on environmental parameters, such as wind and humidity. Based on the graph in Figure 9 and the regression analysis, it can be concluded that freshwater production is not highly dependent on the surrounding wind speed, and it has a constant slope. Conversely, in the graph depicted in Figure 10, freshwater production is directly related to the humidity level, and the slope of these changes is presented in the regression analysis. This increase is due to a rise in relative humidity, which increases the amount of water vapor available for condensation, ultimately leading to a higher production of fresh water. Figure 11 illustrates the changes in the production of fresh water in the desalination unit concerning variations in solar radiation. The graph shows a simultaneous increase in freshwater production with an increase in solar radiation, which signifies a direct relationship between this parameter and water production. The increase in freshwater production is due to the thermal energy caused by radiation, leading to increased evaporation and, as a result, increased freshwater production.

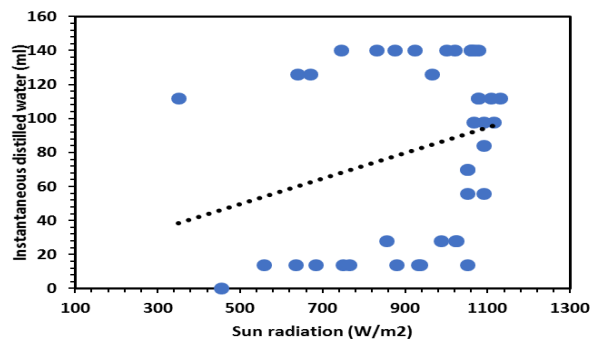


Figure 11. The effect of solar radiation on the production of freshwater

Figure 12 illustrates the instantaneous efficiency graph of the desalination unit during the experiment, while Figure 13 displays the unit's efficiency calculated cumulatively up to the desired moment. Both graphs demonstrate an increase in the unit's efficiency throughout the experiment. Initially, due to the decrease in solar radiation and lower temperatures, less evaporation resulted in lower efficiency levels. However, as solar radiation and air temperature increased over time, evaporation and freshwater also increased, improving efficiency.

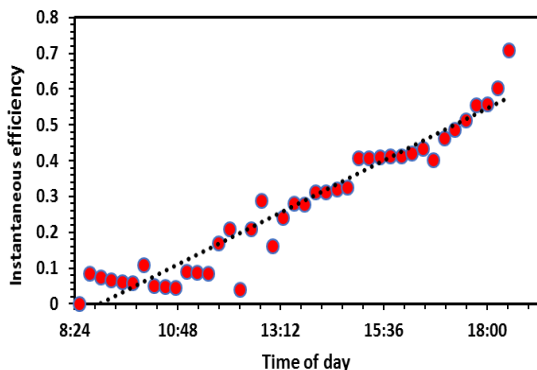


Figure 12. Instantaneous changes in the desalination efficiency graph

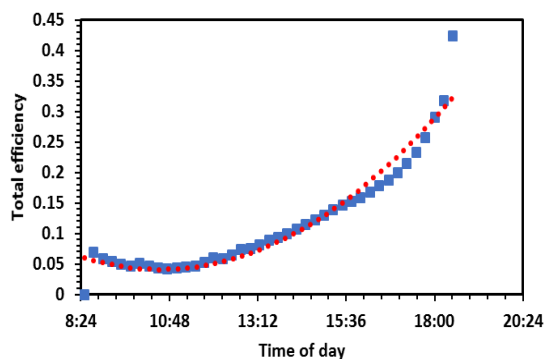


Figure 13. Cumulative changes in desalination efficiency graph

By the end of the day, although the amount of radiation was lower than at noon, the reduction in temperature towards sunset caused previous evaporations to condense, increasing freshwater production and efficiency. Figure 14 illustrates this phenomenon. The unit's average efficiency was 27.1%, with a maximum efficiency of approximately 70%. Table 5 compares the present unit and some previously constructed units.

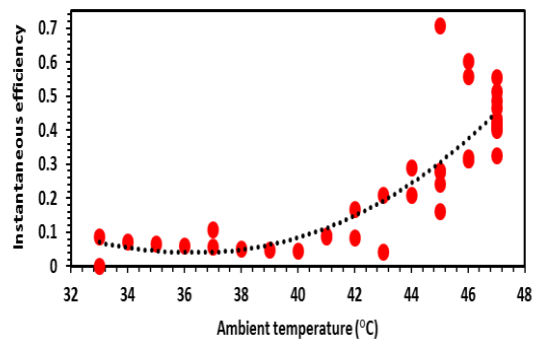


Figure 14. Instantaneous efficiency based on ambient temperature

Table 5. Comparison of the present results with previous researchers

Researcher	Device Production	Device Efficiency	Sweet Water Specifications	Max Error (%)
Omara et al. [23]	3.8 L/day	45%	Conventional Pyramid	1.6
Radomska [10]	Max 9.292 L/m ² /day	21.6% increase due to electric heater	Combination with electric heater	8.3
Abd Elbar et al. [6]	3.534 kg/m ² /day	Max 38.07%	Single-sided with preheating using one	10.0
Agrawal et al. [24]	5.37 kg/m ² /day	Max 41.99%	Sloping flat with one m ² area	1.9
Manokar et al. [13]	6.35 kg/m ² /day	Max 53.95%	Triangle with 0.25 m ² area	10.0
Fathy et al. [25]	10.93 L/m ² /day	26.87%	Double-level Shirvani with 1.5 m ²	3.1
Current study	3.34 L/m ² /day	Average efficiency 27.1%	Six-sided pyramid	5.5

4. Conclusion

The production of freshwater using a six-faced regular pyramid solar water desalination device, designed and built by the authors, was experimentally examined in this study. The device was tested in its base state (inactive) without any activating equipment. The investigations focused on

producing fresh water and the effect of various parameters, including environmental and weather conditions such as temperature, humidity, wind speed, and solar radiation. The results indicated that this type of desalination device can desalinate approximately 3.43 liters of water on a summer day with relatively high humidity. Consequently, the maximum efficiency measured was approximately 70%, and the average daily performance was about 27.1%. Additionally, the results showed that humidity and solar radiation are directly related to the increase in water desalination. by increasing use of fresh water in 3D dimensional solar desalination, we can hope to combine these systems with energy storage and water storage systems in the future.

Nomenclature

A_c	Surface area of solar distiller (m^2)
E	Energy (J)
G	Sun radiation (W/m^2)
L_f	Latent heat of evaporation (kJ/kg)
m_w	Distilled water mass (kg)
q_{ev}	Evaporating heat transfer (J)
Q_U	Output energy (J)
ΔT	Temperature difference ($^{\circ}C$)
Δt	Time difference (S)
η	Efficiency
τ_w	Water transmittance coefficient
τ_g	Glass transmittance coefficient
α_p	Absorption coefficient of adsorbent

References

- [1] Manchanda, H., & Kumar, M. (2022). Performance evaluation of a locally designed stepped solar distillation-cum-active drying unit. *Journal of Thermal Analysis and Calorimetry*, 147(6), 4383-4395. <https://doi.org/doi.org/10.1007/s10973-021-10835-x>
- [2] Moravej, M. (2021). An experimental study of the performance of a solar flat plate collector with triangular geometry. *Journal of Solar Energy Research*, 6(4), 923-936. doi:10.22059/JSER.2020.311364.1178
- [3] Moravej, M., & Namdarnia, F. (2018). Experimental investigation of the efficiency of a semi-spherical solar piping collector. *Journal of Renewable Energy and Environment*, 5(2), 22-30. <https://doi.org/doi.org/10.30501/jree.2018.88602>
- [4] Attia, M. E. H., El-Maghlany, W. M., Abdelgaied, M., & Elharidi, A. M. (2022). Finest concentration of phosphate grains as energy storage medium to improve hemispherical solar distillate: An experimental study. *Alexandria Engineering Journal*, 61(7), 5573-5583. <https://doi.org/doi.org/10.1016/j.aej.2021.11.014>
- [5] Ezzarrouqy, K., Hejjaj, A., Idlimam, A., Nouh, F. A., & Mandi, L. (2022). Study of the energetic, exergetic, and thermal balances of a solar distillation unit in comparison with a conventional system during the distillation of rosemary leaves. *Environmental Science and Pollution Research*, 29(17), 25709-25722. <https://doi.org/doi.org/10.1007/s11356-021-17612-1>
- [6] Abd Elbar, A. R., & Hassan, H. (2020). Enhancement of hybrid solar desalination system composed of solar panel and solar still by using porous material and saline water preheating. *Solar Energy*, 204, 382-394. <https://doi.org/doi.org/10.1016/j.solener.2020.04.058>
- [7] Zanganeh, P., Goharrizi, A. S., Ayatollahi, S., Feilizadeh, M., & Dashti, H. (2020). Efficiency improvement of solar stills through wettability alteration of the condensation surface: An experimental study. *Applied energy*, 268, 114923. <https://doi.org/doi.org/10.1016/j.apenergy.2020.114923>
- [8] Modi, K. V., & Nayi, K. H. (2020). Efficacy of forced condensation and forced evaporation with thermal energy storage material on square pyramid solar still. *Renewable energy*, 153, 1307-1319. <https://doi.org/doi.org/10.1016/j.renene.2020.02.095>
- [9] Saravanan, A., & Murugan, M. (2020). Performance evaluation of square pyramid solar still with various vertical wick

- materials—an experimental approach. *Thermal Science and Engineering Progress*, 19, 100581. <https://doi.org/doi.org/10.1016/j.tsep.2020.100581>
- [10] Radomska, E., Mika, L., Sztékler, K., & Kalawa, W. (2021). Experimental validation of the thermal processes modeling in a solar still. *Energies*, 14(8), 2321. <https://doi.org/doi.org/10.3390/en14082321>
- [11] Poonia, S., Singh, A., & Jain, D. (2020). Design development and performance evaluation of concentrating solar thermal desalination device for hot arid region of India. *Desalination and Water Treatment*, 205, 1-11. <https://doi.org/doi:10.5004/dwt.2020.26381>
- [12] Abed, F. M., Eleiwi, M. A., Hasanuzzaman, M., Islam, M., & Mohammed, K. I. (2020). Design, development and effects of operational conditions on the performance of concentrated solar collector based desalination system operating in Iraq. *Sustainable Energy Technologies and Assessments*, 42, 100886. <https://doi.org/doi.org/10.1016/j.seta.2020.100886>
- [13] Muthu Manokar, A., Prince Winston, D., Sathyamurthy, R., Kabeel, A., & Rama Prasath, A. (2019). Experimental investigation on pyramid solar still in passive and active mode. *Heat and Mass Transfer*, 55, 1045-1058. <https://doi.org/doi.org/10.1007/s00231-018-2483-3>
- [14] Kabeel, A. E., Abdelgaied, M., & Almulla, N. (2016). Performances of pyramid-shaped solar still with different glass cover angles: experimental study. 2016 7th International Renewable Energy Congress (IREC), doi.10.1109/IREC.2016.7478869
- [15] Chaichan, M. T., Kazem, H. A., Abaas, K. I., & Al-Waeli, A. A. (2016). Homemade solar desalination system for Omani families. *International Journal of Scientific & Engineering Research*, 7(5), 1499-1504.
- [16] Siva Sankaran, N., & Sridharan, M. (2022). Experimental research and performance study of double slope single basin solar distillation still using CFD techniques. *International Journal of Ambient Energy*, 43(1), 3796-3803. <https://doi.org/doi.org/10.1080/01430750.2020.1852109>
- [17] Shakerian, M., Karrabi, M., Gheibi, M., Fathollahi-Fard, A. M., & Hajiaghaei-Keshteli, M. (2022). Evaluating the Performance of a Solar Distillation Technology in the Desalination of Brackish Waters. *Processes*, 10(8), 1626. <https://doi.org/doi.org/10.3390/pr10081626>
- [18] Kumar, M. M., Rajesh, S., Appadurai, M., & Gnanaraj, S. J. P. (2022). Performance enhancement of solar distillation system with internal modification. *Materials Today: Proceedings*, 62, 5452-5455. <https://doi.org/doi.org/10.1016/j.matpr.2022.04.116>
- [19] Naghdi, B., Roghabadi, F. A., & Soleimani-Gorgani, A. (2024). Salt-resistant solar water desalination system via surface modification and configuration engineering. *Desalination*, 577, 117390. <https://doi.org/https://doi.org/10.1016/j.desal.2024.117390>
- [20] Senthilkumar, N., Deepanraj, B., Sundar, L. S., & Ravikumar, N. (2024). Optimizing the Productivity of Solar Water Desalination System Using Firefly Algorithm. 2024 Third International Conference on Intelligent Techniques in Control, Optimization and Signal Processing (INCOS), doi: IEEE. 10.1109/INCOS59338.2024.10527668
- [21] Mohammed, R. H., Qasem, N. A., Farid, A., Zubair, S. M., Alsaman, A. S., Askalany, A. A., & Ali, E. S. (2023). A novel solar-powered thermal desalination unit coupled with a reverse osmosis plant to increase overall water recovery. *Applied Thermal Engineering*, 234, 121306. <https://doi.org/https://doi.org/10.1016/j.applthermaleng.2023.121306>
- [22] Zhang, S., Wang, J., Zhao, B., Zhou, L., Liu, N., Lan, Q., & Liu, J. (2024). A self-floating integrated hydrogel evaporator with efficient salt resistance and thermal localization for efficient solar water desalination. *Chemical Engineering Journal*, 152302. <https://doi.org/https://doi.org/10.1016/j.cej.2024.152302>
- [23] Omara, Z., Alawee, W. H., Mohammed, S. A., Dhahad, H. A., Abdullah, A., & Essa, F. A. (2022). Experimental study on the performance of pyramid solar still with

novel convex and dish absorbers and wick materials. *Journal of Cleaner Production*, 373, 133835. <https://doi.org/doi.org/10.1016/j.jclepro.2022.133835>

- [24] Agrawal, A., Rana, R., & Srivastava, P. K. (2017). Heat transfer coefficients and productivity of a single slope single basin solar still in Indian climatic condition: Experimental and theoretical comparison. *Resource-Efficient Technologies*, 3(4), 466-482. <https://doi.org/doi.org/10.1016/j.reffit.2017.05.003>
- [25] Fathy, M., Hassan, H., & Ahmed, M. S. (2018). Experimental study on the effect of coupling parabolic trough collector with double slope solar still on its performance. *Solar Energy*, 163, 54-61. <https://doi.org/doi.org/10.1016/j.solener.2018.01.043>